

Electronically Selective Chemical Functionalization of Carbon Nanotubes: Correlation between Raman Spectral and Electrical Responses

Congjun Wang,^{*,†} Qing Cao,[‡] Taner Ozel,[§] Anshu Gaur,^{†,||} John A. Rogers,^{†,‡,||} and Moonsub Shim^{*,†}

Contribution from the Department of Materials Science and Engineering, Department of Chemistry, Department of Physics, Beckman Institute and Frederick Seitz Materials Research Laboratory, University of Illinois at Urbana–Champaign, Urbana, Illinois 61801

Received April 24, 2005; E-mail: congjun@uiuc.edu; mshim@uiuc.edu

Abstract: Single-walled carbon nanotubes (SWNTs) demonstrate remarkable electronic and mechanical properties useful in developing areas such as nanoelectromechanical systems and flexible electronics. However, the highly inhomogeneous electronic distribution arising from different diameters and chirality in any given as-synthesized SWNT samples imposes severe limitations. Recently demonstrated selective chemical functionalization methods may provide a simple scalable means of eliminating metallic tubes from SWNT transistors and electronic devices. Here, we report on combined electron transport and Raman studies on the reaction of 4-bromobenzene diazonium tetrafluoroborate directly with single and networks of SWNT transistors. First, Raman studies are carried out on isolated individual SWNTs grown on SiO₂/Si substrates by chemical vapor deposition with and without metal contacts. Metallic tubes are found to have, on average, higher reactivity toward diazonium reagents. However, a considerable degradation of electrical properties of semiconducting tubes occurs if the reaction is carried out to the point where the conductivity of metallic tubes is significantly suppressed. Insights from single-tube studies are then applied to elucidate the electrical and the Raman responses of SWNT random network transistors of different channel lengths to chemical functionalization.

Introduction

Single-walled carbon nanotubes (SWNTs) exhibit exceptional electronic properties including extremely high hole mobilities ($\sim 100\,000\text{ cm}^2/\text{Vs}$),¹ current carrying capacity exceeding 10^9 A/cm^2 ,² simple electrostatic current modulation with ON current to OFF current ratio (ON/OFF ratio) larger than 10^5 ,³ and ballistic transport^{4–6} with mean free path on the order of a micrometer. Together with their mechanical robustness⁷ and the ease of direct printing onto plastic substrates,⁸ SWNT networks or arrays are promising materials for applications especially in developing technologies such as large-area flexible thin film transistors (TFTs). Hole mobilities near $100\text{ cm}^2/\text{Vs}$ or higher,

which is about 100 times larger than that of the best organic TFTs, have been demonstrated in SWNT TFTs.^{9,10} However, this high mobility is still well below the ideal limit considering high performances observed in individual SWNT transistors.¹ Another shortcoming of SWNT TFTs is the decreasing ON/OFF ratio as the channel length decreases which prevents miniaturization beyond average tube length which is typically in the micrometer range. One of the main reasons for these limited performances of SWNT TFTs is the substantial number of metallic tubes in the SWNT mixtures generated by any current growth methods. Separating metallic and semiconducting SWNTs has therefore been a central issue for most electronics applications including high-performance TFTs.

Recently, several key progresses have been made toward achieving electronic homogeneity. The use of Co–Mo catalyst¹¹ and plasma-enhanced chemical vapor deposition (CVD)¹² have been reported to lead to an enrichment or a significant preference of semiconducting SWNTs. Several postsynthesis approaches to selectively eliminate metallic SWNTs have also been

[†] Department of Materials Science and Engineering.

[‡] Department of Chemistry.

[§] Department of Physics.

^{||} Beckman Institute and Frederick Seitz Materials Research Laboratory.

- (1) Durkop, T.; Getty, S. A.; Cobas, E.; Fuhrer, M. S. *Nano Lett.* **2004**, *4*, 35–39.
- (2) Yao, Z.; Kane, C. L.; Dekker, C. *Phys. Rev. Lett.* **2000**, *84*, 2941–2944.
- (3) Javey, A.; Kim, H.; Brink, M.; Wang, Q.; Ural, A.; Guo, J.; McIntyre, P.; McEuen, P.; Lundstrom, M.; Dai, H. *Nature Mater.* **2002**, *1*, 241–246.
- (4) Javey, A.; Guo, J.; Wang, Q.; Lundstrom, M.; Dai, H. *Nature* **2003**, *424*, 654–657.
- (5) Liang, W.; Bockrath, M.; Bozovic, D.; Hafner, J. H.; Tinkham, M.; Park, H. *Nature* **2001**, *411*, 665–669.
- (6) Frank, S.; Poncharal, P.; Wang, Z. L.; de Heer, W. A. *Science* **1998**, *280*, 1744–1746.
- (7) Wong, E. W.; Sheehan, P. E.; Lieber, C. M. *Science* **1997**, *277*, 1971–1975.
- (8) Meitl, M. A.; Zhou, Y.; Gaur, A.; Jeon, S.; Usrey, M. L.; Strano, M. S.; Rogers, J. A. *Nano Lett.* **2004**, *4*, 1643–1647.

- (9) Snow, E. S.; Novak, J. P.; Campbell, P. M.; Park, D. *Appl. Phys. Lett.* **2003**, *82*, 2145–2147.
- (10) Zhou, Y.; Gaur, A.; Hur, S.-H.; Kocabas, C.; Meitl, M. A.; Shim, M.; Rogers, J. A. *Nano Lett.* **2004**, *4*, 2031–2035.
- (11) Bachilo, S. M.; Balzano, L.; Herrera, J. E.; Pompeo, F.; Resasco, D. E.; Weisman, R. B. *J. Am. Chem. Soc.* **2003**, *125*, 11186–11187.
- (12) Li, Y.; Mann, D.; Rolandi, M.; Kim, W.; Ural, A.; Hung, S.; Javey, A.; Cao, J.; Wang, D.; Yenilmez, E.; Wang, Q.; Gibbons, J. F.; Nishi, Y.; Dai, H. *Nano Lett.* **2004**, *4*, 317–321.

developed. One method is the electrical breakdown of metallic tubes which may be effective but limited to one or a very small number of devices at a time.^{10,13} Chemical functionalization of SWNTs with dichlorocarbene,¹⁴ octadecylamine,¹⁵ nitronium ions,¹⁶ and phenyl diazonium compounds,¹⁷ which may lead to scalable routes to achieving electronic homogeneity, have also been reported. For direct application in SWNT network or array TFTs, covalent functionalization with preferential reactivity toward metallic tubes may be the most desirable. Such a selective reactivity would allow postfabrication removal of metallic contributions to the conductivity that would otherwise cause electrical shorting and performance degradation of network or array TFTs. In this regard, the reaction with diazonium compounds¹⁷ provides one of the most convenient methods along with mild reaction conditions and readily available reagents. The proposed mechanism for the origin of the chemical selectivity is that the finite electronic density of states near the Fermi level in metallic tubes stabilizes the charge-transfer complex and facilitates the reaction. On the other hand, the zero density of states at the Fermi level in semiconducting tubes results in a slower reaction rate.¹⁷

One of the main drives for developing simple scalable chemistries for separating metallic and semiconducting SWNTs is to exploit their exceptional properties in electronic devices. Hence the report of preferential reactivity of diazonium reagents to metallic SWNTs¹⁷ is prompting many efforts in integrating this chemical process to improve performance of SWNT devices. Recently, two studies of covalent functionalization of SWNT devices with benzene diazonium derivatives have been reported. The first approach has utilized an applied electrochemical potential to initiate the reaction between SWNTs and 4-nitrobenzene diazonium salt with prior charging of the devices by an applied back gate voltage.¹⁸ After the selective functionalization, an increase in the ON/OFF ratio from 3 to $\sim 10^6$ accompanied by a similar amount of reduction in both ON ($\sim 7\text{-}\mu\text{S}$ decrease) and OFF ($\sim 3\text{-}\mu\text{S}$ decrease) conductance has been observed. Initial devices in this method contained only a couple of bundles of nanotubes that directly spanned the channel between the drain and the source electrodes. The performance improvement of the resultant system is most likely from having a transistor with a very small number of tubes where there happens to be a large enough difference in the reactivity between the limited number of metallic and semiconducting tubes. In a large ensemble, a reactivity distribution and therefore an overlap in the degree of conductivity suppression via covalent functionalization of metallic and semiconducting tubes is likely which can lead to less than optimal performance improvements. Chemical functionalization in the second method has been carried out simply by placing a drop of 4-bromobenzene diazonium tetrafluoroborate solution on top of a network of electrically contacted SWNTs, and the selectivity is reported

to be achieved at an optimum concentration.¹⁹ An ON/OFF ratio of about 10^3 with very little or no reduction in the ON current has been reported with this method. We note that, in this second case, the reported devices that showed the optimum result initially had a very small gate dependence (i.e., the initial ON/OFF ratio is only about 1.5 or less within a very large gate voltage range of 110 V as shown in Figures 2 and 3 of ref 19).

The efficiency of the diazonium chemistry in improving the ON/OFF ratios of multitube transistors is clear from both studies.^{18,19} However, there is a need for a better understanding of how covalent bond formation leads to performance improvement of a rather complex network. In general, no clear relation has been established between chemical reactions (whether intentional or inevitable from processing requirements) and their effects on the electron transport properties, but this relation is central to most electronic applications of SWNTs. From isolated individual tubes to complex networks, there are no simple scaling guidelines that can be followed to predict the electrical behavior upon covalent functionalization. For these purposes, a more comprehensive set of measurements that goes beyond probing global electrical conductance change is necessary. Factors such as the substrate and metal contacts present large deviations in the reaction conditions and adapting chemistry developed for solution-phase reaction in the presence of surfactants may not be straightforward. To elucidate these critical issues of how chemistry alters electron-transport properties of individual and networks of SWNTs, we combine electrical and Raman spectroscopic measurements to examine the reaction of diazonium reagents with SWNT transistors. Differences in the reactivity of isolated metallic and semiconducting tubes with and without electrical contacts are first established. Comparisons between Raman spectral and electrical responses are made in order to correlate the degree of chemical reaction with changes in the electrical conductivity of individual tubes. These results are then applied to explain and to optimize the effects of the diazonium chemistry on the electrical conductivity of random networks of SWNTs with different transistor channel lengths.

Experimental Section

Individual SWNT transistors were prepared by a patterned CVD method.²⁰ Fe/alumina catalyst (15 mg $\text{Fe}(\text{NO}_3)_3 \cdot 9\text{H}_2\text{O}$ and 20 mg Al_2O_3 powder suspended in 20 mL of methanol) was patterned on SiO_2/Si substrates by spin casting and liftoff. Growth of SWNTs was carried out at 900 °C with ultrahigh purity CH_4 and H_2 as the carbon feedstock and the dilution gas, respectively. Metal contacts (3 nm of Ti with 50 nm of Au) were evaporated on top of SWNTs. Photolithography steps utilized poly(methyl methacrylate) as the resist with deep UV exposure and a $\sim 400\text{-nm}$ SiO_2 served as the gate dielectric. Short channel length (1 μm) SWNT TFTs were also fabricated using the same CVD method but with ferritin catalysts. The ferritin catalyst was placed on patterned areas slightly larger than the channel region using photolithography with Shipley 1805 photoresist. The metal contacts were evaporated on top of SWNTs in the same manner as the individual SWNT transistors. Long channel length (55 μm) SWNT TFTs were fabricated using the same method as the short channel devices except that the ferritin catalysts were not patterned. Stripes in the SWNT films were made with O_2 -reactive ion etching after a photolithography step using Shipley 1805 resist.¹⁰ The width and the spacing of the stripes are $\sim 5\ \mu\text{m}$. This striping step minimizes gate leakage which occurs mainly due to

(13) Collins, P. G.; Arnold, M. S.; Avouris, Ph. *Science* **2001**, *292*, 706–709.

(14) Kamaras, K.; Itkis, M. E.; Hu, H.; Zhao, B.; Haddon, R. C. *Science* **2003**, *301*, 1501.

(15) Chattopadhyay, D.; Galeska, I.; Papadimitrakopoulos, F. *J. Am. Chem. Soc.* **2003**, *125*, 3370–3375.

(16) An, K. H.; Park, J. S.; Yang, C.-M.; Jeong, S. Y.; Lim, S. C.; Kang, C.; Son, J.-H.; Jeong, M. S.; Lee, Y. H. *J. Am. Chem. Soc.* **2005**, *127*, 5196–5203.

(17) Strano, M. S.; Dyke, C. A.; Usrey, M. L.; Barone, P. W.; Allen, M. J.; Shan, H.; Kittrell, C.; Hauge, R. H.; Tour, J. M.; Smalley, R. E. *Science* **2003**, *301*, 1519–1522.

(18) Balasubramanian, K.; Sordan, R.; Burghard, M.; Kern, K. *Nano Lett.* **2004**, *4*, 827–830.

(19) An, L.; Fu, Q.; Lu, C.; Liu, J. *J. Am. Chem. Soc.* **2004**, *126*, 10520–10521.

(20) Kong, J.; Soh, H. T.; Cassell, A. M.; Quate, C. F.; Dai, H. *Nature* **1998**, *395*, 878–881.

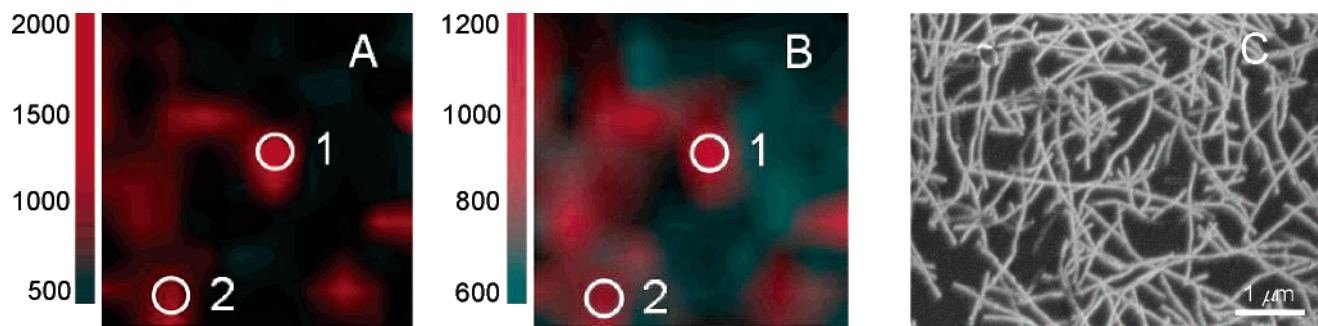


Figure 1. Raman maps of the tangential mode of pristine SWNTs before (A) and after (B) functionalization with 10 μM diazonium solution for 10 min. Both images are $10 \times 10 \mu\text{m}^2$. (C) SEM image of the SWNT film.

tube growth over the edges of the substrate and also eliminates cross-talk between devices.^{10,21}

For chemical functionalization, a drop of the 4-bromobenzene diazonium tetrafluoroborate (4-BBDT, Aldrich) in 10^{-4} M NaOH solution was placed on top of the SWNT devices and allowed to react for 10 min at room temperature. The devices were then thoroughly rinsed with deionized water and heated to 100 °C in air for ~ 2 min to remove solvents before electrical measurements in the back gate configuration. No noticeable reaction was observed to take place at concentrations below 1 μM . For concentration dependence, reactions and annealing steps were carried out from the lowest to the highest concentrations in the same manner with electrical and Raman measurements between concentrations. For the concentration range studied here, all changes in the Raman spectra and electron transport characteristics occurred within the first few minutes. Therefore the 10-min reaction period was chosen to ensure the completion of the reaction for each concentration. We have also examined chemical functionalization where the reagents are introduced through a microfluidic channel directly over the SWNT devices. No differences were seen whether the reaction was carried out with a drop of solution placed on top of the devices or in the microfluidic channels. With microfluidic delivery of chemicals, electrochemical gating^{22–26} (using a Ag/AgCl reference electrode) can be used to apply a solution potential as well as to allow a real-time electrical monitoring of the reactions. It also allows measurements without postreaction annealing. The same qualitative responses were observed whether we measured the devices with electrochemical gating directly after the reaction or with back gating after 100 °C annealing. For the subsequent discussion, only the results from reactions without the microfluidic channels are considered for clarity.

Raman measurements were performed with a Jobin Yvon HR 800 micro-Raman spectrometer at 633-nm excitation before and after chemical functionalization. The laser beam was focused onto the sample with a 100 \times objective. The laser intensity at the sample was kept below the threshold for any laser-induced changes in the Raman spectra²⁷ and electrical transport characteristics. Electrical measurements were carried out with Agilent 4156C high precision semiconductor parameter analyzer. Scanning electron microscopy (SEM) and atomic force microscopy (AFM) images were collected with a Hitachi S4700 SEM and a Digital Instruments Dimension 3100 AFM, respectively.

Results and Discussion

Especially because of the all-surface atom makeup of SWNTs, electron transport is highly environment sensitive (often without

much selectivity) as exemplified by the large electrical response to many different gases^{28,29} and polymers³⁰ as well as by the large hysteresis^{31–34} commonly observed in SWNT transistors. In functionalizing SWNT devices, it may be inevitable to expose the chemical reagents to immediate surroundings of the nanotube leading to possible variations in the contacts as well as the substrate contributing to the observed changes in the electrical conductance. How the devices are prepared (e.g., deposition of surfactant suspended SWNTs vs direct growth on substrates) may also have significant effects. As shown later, even the differences in the channel lengths of the SWNT network devices can alter the overall electrical response to the chemical reaction. Therefore, it is critical to have independent measurements that can monitor, for example, by Raman spectroscopy,³⁵ changes occurring directly on SWNTs along with conductance measurements to elucidate the “on-chip” selective chemical functionalization process.

We first discuss Raman measurements on SWNTs that are *not* integrated into transistors to establish the spectroscopic signature brought on by the reaction with 4-BBDT without possible complications from contact metals or residues from lithography. Combined electrical and spectroscopic changes observed in individual SWNT transistors are then discussed to elucidate the differences between the reactivity and the electrical responses of metallic and semiconducting tubes. With insights from single-tube measurements, how performance of SWNT network TFTs improves or degrades with chemical functionalization is discussed.

Changes in the Raman Spectra of “Pristine” SWNTs. Parts A and B of Figure 1 show the same area Raman map of the tangential mode ($1575\text{--}1610 \text{ cm}^{-1}$) of a random array of SWNTs on SiO_2/Si substrate before and after reaction with 4-BBDT. There are no metal contacts, and no lithography steps have been taken on these samples. The CVD growth is taken

- (21) Ozel, T.; Gaur, A.; Rogers, J. A.; Shim, M. *Nano Lett.* **2005**, *5*, 905–911.
 (22) Krüger, M.; Buitelaar, M. R.; Nussbaumer, T.; Schönenberger, C.; Forró, L. *Appl. Phys. Lett.* **2001**, *78*, 1291–1293.
 (23) Rosenblatt, S.; Yaish, Y.; Park, J.; Gore, J.; Sazonova, V.; McEuen, P. L. *Nano Lett.* **2002**, *2*, 869–872.
 (24) Siddons, G. P.; Merchin, D.; Back, J. H.; Jeong, J. K.; Shim, M. *Nano Lett.* **2004**, *4*, 927–931.
 (25) Lu, C.; Fu, Q.; Huang, S.; Liu, J. *Nano Lett.* **2004**, *4*, 623–627.
 (26) Heller, I.; Kong, J.; Heering, H. A.; Williams, K. A.; Lemay, S. G.; Dekker, C. *Nano Lett.* **2005**, *5*, 137–142.
 (27) Yu, Z.; Brus, L. E. *J. Phys. Chem. A* **2000**, *104*, 10995–10999.

- (28) Kong, J.; Franklin, N. R.; Zhou, C.; Chapline, M. G.; Peng, S.; Cho, K.; Dai, H. *Science* **2000**, *287*, 622–625.
 (29) Shim, M.; Siddons, G. P. *Appl. Phys. Lett.* **2003**, *83*, 3564–3566.
 (30) Shim, M.; Javey, A.; Kam, N. W. S.; Dai, H. *J. Am. Chem. Soc.* **2001**, *123*, 11512–11513.
 (31) Fuhrer, M. S.; Kim, B. M.; Durkop, T.; Brintlinger, T. *Nano Lett.* **2002**, *2*, 755–759.
 (32) Radosevljevi, M.; Freitag, M.; Thadani, K. V.; Johnson, A. T. *Nano Lett.* **2002**, *2*, 761–764.
 (33) Cui, J. B.; Sordan, R.; Burghard, M.; Kern, K. *Appl. Phys. Lett.* **2002**, *81*, 3260–3262.
 (34) Kim, W.; Javey, A.; Vermesh, O.; Wang, Q.; Li, Y.; Dai, H. *Nano Lett.* **2003**, *3*, 193–198.
 (35) (a) Rao, A. M.; Richter, E.; Bandow, S.; Chase, B.; Eklund, P. C.; Williams, K. A.; Fang, S.; Subbaswamy, K. R.; Menon, M.; Thess, A.; Smalley, R. E.; Dresselhaus, G.; Dresselhaus, M. S. *Science* **1997**, *275*, 187–191. (b) Dresselhaus, M. S.; Dresselhaus, G.; Jorio, A.; Filho, A. G. S.; Pimenta, M. A.; Saito, R. *Acc. Chem. Res.* **2002**, *35*, 1070–1078. (c) Hartschuh, A.; Pedrosa, H. N.; Novotny, L.; Krauss, T. D. *Science* **2003**, *301*, 1354.

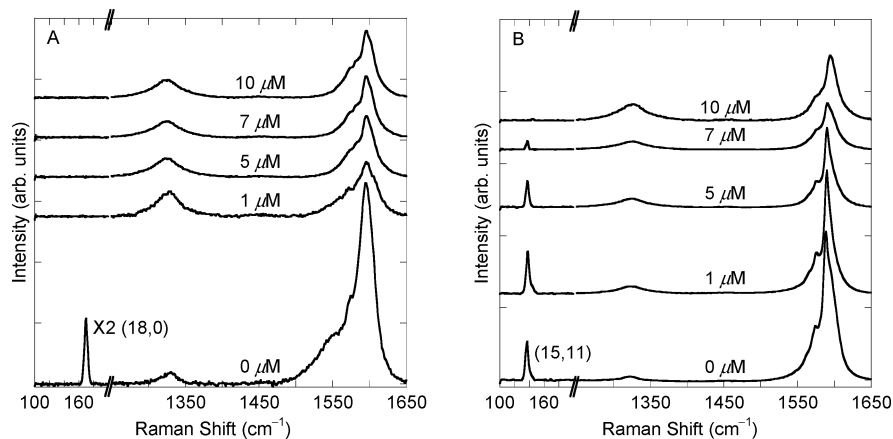


Figure 2. (A) Raman spectra at spot 1 on the pristine SWNT film shown in parts A and B of Figure 1 after reacting with different concentrations of 4-BBDT in $\sim 10^{-4}$ M NaOH solution for ~ 10 min. (B) Raman spectra at spot 2 in parts A and B of Figure 1 after functionalization at different concentrations of 4-BBDT solutions.

as the last step in the sample preparation to allow us to examine the effects on “pristine” tubes. From the SEM image in Figure 1C, the average tube density is $\sim 3 \mu\text{m}^{-2}$. The laser spot diameter is $\sim 1 \mu\text{m}$, and each spot seen in the Raman map corresponds to one or a very few number of tubes. The appearance of only one radial breathing mode (RBM) in the low-frequency range for a given spot further supports this claim.

Figure 2A shows the Raman spectra at the spot labeled 1 in parts A and B of Figure 1 before and after the reaction with 4-BBDT at different concentrations as indicated. The intensities of the spectra are normalized to the substrate Si Raman peak at $\sim 940 \text{ cm}^{-1}$ (not shown for clarity). Following refs 36–38, we assign this tube with RBM at 169 cm^{-1} to be a (18,0) SWNT and therefore a metallic SWNT. Technically, this would be a small band gap tube when the curvature is taken into account.³⁹ However, since the energy gaps of nonarmchair small gap tubes are much smaller than the room temperature thermal energy, we refer to all tubes as metallic if the (n,m) index difference is integer multiple of 3.

There are three distinct changes in the Raman spectra upon reaction with 4-BBDT. Even at a relatively low concentration of $1 \mu\text{M}$, the appearance of the disorder mode (DM) at $\sim 1300 \text{ cm}^{-1}$ and a decrease in the intensity of the tangential mode (TM) at $\sim 1590 \text{ cm}^{-1}$ with simultaneous disappearance of the RBM at 169 cm^{-1} can be seen for the tube in Figure 2A. These changes are consistent with measurements carried out on SWNTs suspended in aqueous solutions with surfactants.¹⁷ As covalent bonds are made with 4-BBDT, π conjugation in SWNTs begins to be disrupted. With the decreased number of sp^2 -hybridized carbon atoms, a loss of crystallinity is indicated by the appearance of the DM in the Raman spectrum. Interestingly, the disappearance of the RBM and the decrease in the intensity of the TM are not accompanied by line broadening or frequency shifts. This may support the idea that, once a carbon atom in a SWNT has reacted, the neighboring carbon atoms are likely to have increased reactivity to subsequent reactions with 4-BBDT.¹⁷ That is, covalent bond formation occurs in patches leading to unreacted segments that maintain RBM and

TM of the initial tube. No significant changes are seen upon further reaction at higher concentrations up to 1 mM 4-BBDT solution.

Figure 2B shows the Raman spectra from the spot labeled 2 in parts A and B of Figure 1. The RBM is at 137 cm^{-1} corresponding to a (15,11) SWNT, which is a semiconducting tube. Similar changes (i.e., the appearance of the DM, the decrease in the TM intensity, and the loss of the RBM) as the metallic tube in spot 1 can be seen at the higher concentration of $10 \mu\text{M}$ 4-BBDT. However, unlike the metallic tube, this semiconducting tube shows no significant changes in the RBM, TM, and DM at the low concentration of $1 \mu\text{M}$ 4-BBDT. Rather, there is a gradual decrease in both the RBM and the TM along with a gradual increase in the DM at higher concentrations. This difference in the concentration dependence of the semiconducting and the metallic tubes confirms electronically selective reactivity of 4-BBDT and indicates feasibility of this chemical process for SWNTs grown directly on SiO_2/Si substrates suitable for device fabrication. However, as shown and discussed later, there is a significant spread in the reactivity of different chirality tubes suggesting that there may be a limit to the improvement in the device performance.

Response of Single-Tube Transistors. As expected from Raman studies of low-density SWNTs on SiO_2/Si substrates, individual SWNTs contacted with metal electrodes exhibit similar responses to reaction with 4-BBDT. Figure 3A shows the changes in the Raman spectrum of an individual SWNT transistor. The inset in Figure 3B is an AFM image of the device. Figure 3B shows the electron-transport characteristics of this device indicating no significant modulation of current with back gate as expected for a metallic tube. Upon reaction with $1 \mu\text{M}$ 4-BBDT, there is a significant decrease in the conductance from 1.0 to $0.4 \mu\text{S}$. The appearance of the DM and the decrease in the intensity of TM (Figure 3A) are accompanied by this decrease in the conductance. However, the decrease in the conductivity does not seem to change the metallic behavior of the tube as indicated by the gate-independent conductance, which is maintained up to the highest concentration we have employed (1 mM). Surprisingly, there is very little change in both Raman and electrical conductivity from $10 \mu\text{M}$ to 1 mM 4-BBDT. After the reaction at $10 \mu\text{M}$, the 2 orders of magnitude decrease in the electrical conductance for the device

(36) Strano, M. S. *J. Am. Chem. Soc.* **2003**, *125*, 16148–16153.

(37) Murakami, Y.; Miyauchi, Y.; Chiashi, S.; Maruyama, S. *Chem. Phys. Lett.* **2003**, *377*, 49–54.

(38) Jorio, A.; Saito, R.; Hafner, J. H.; Lieber, C. M.; Hunter, M.; McClure, T.; Dresselhaus, G.; Dresselhaus, M. S. *Phys. Rev. Lett.* **2001**, *86*, 1118–1121.

(39) Kane, C. L.; Mele, E. J. *Phys. Rev. Lett.* **1997**, *78*, 1932–1935.

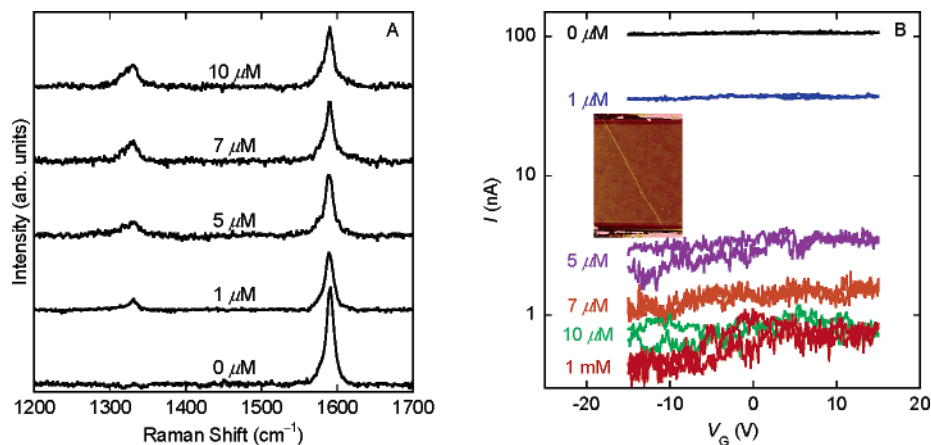


Figure 3. (A) Raman spectra of a single metallic SWNT before and after chemical functionalization. The disorder mode peak at $\sim 1300\text{ cm}^{-1}$ appeared after functionalization. (B) Gate voltage (V_G) independent current (I) for a single metallic SWNT device before and after exposure to various concentrations of diazonium solution for 10 min. Measurements were carried out at a bias of 100 mV. The inset is the AFM image of the device with electrode spacing of $4\ \mu\text{m}$.

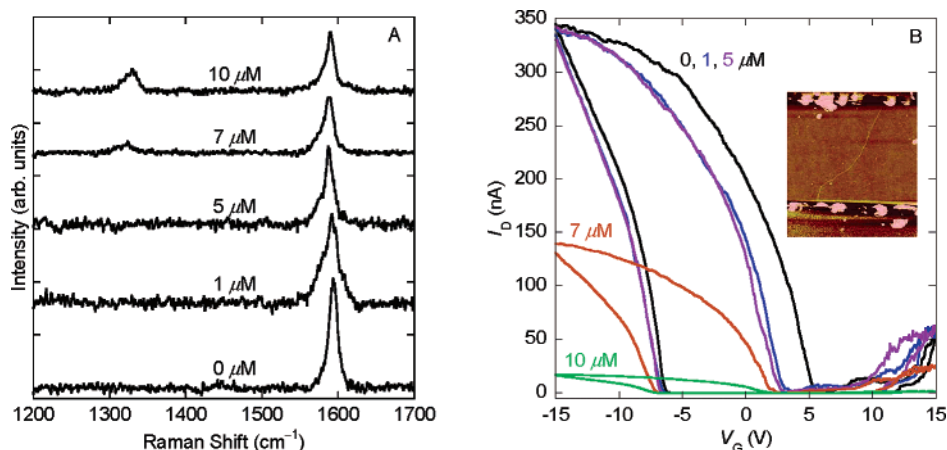


Figure 4. (A) The Raman spectra of a single semiconducting SWNT before and after chemical functionalization at the indicated concentrations. (B) Transfer characteristics of the single semiconducting SWNT device before and after the reaction with 4-BBDT solution. Electrical measurements were carried out in the back gate geometry with $V_{DS} = 100\text{ mV}$. The inset is the AFM image of the device with electrode spacing of $4\ \mu\text{m}$.

shown in Figure 3 is the largest we have observed for isolated metallic tubes. Two other individual metallic tube samples that we have examined show only about 1 order of magnitude decrease at the same concentration. While this decrease is significant, there is still a non-negligible conductivity of metallic tubes after the reaction at $10\ \mu\text{M}$.

Parts A and B of Figure 4 show the Raman and the electrical responses of another individual SWNT transistor. Again, the AFM image (Figure 4B inset) indicates that only a single tube spans the channel and that both Raman and electrical signals arise from this single tube. Large modulation of the drain current from $\sim 350\text{ nA}$ to depletion by electrostatic gate shows that this is a semiconducting tube (Figure 4B). This device also shows a small n-channel conductance at positive gate voltages. Unlike the metallic tube in Figure 3, no significant changes are observed after the reaction with relatively low concentrations of 4-BBDT (up to $\sim 5\ \mu\text{M}$) as indicated by both Raman and electron transport measurements. At $7\ \mu\text{M}$ and higher concentrations of 4-BBDT, there is a significant decrease in the ON current accompanied by the appearance of the DM and a decrease in the TM intensity in the Raman spectrum (Figure 4A). Both p- and n-channel conductance decreases upon covalent functionalization. All semiconducting single-tube devices that we have

measured show p-channel ON current decrease by a factor of $\sim 2\text{--}4$ with reaction at $7\ \mu\text{M}$ and by about 1 order of magnitude at $10\ \mu\text{M}$.

Distribution of Reactivity of SWNTs to 4-BBDT. From the results above, both pristine and electrically contacted tubes show similar selectivity of reaction with diazonium reagents. While these results are promising, there may be a distribution of reactivity of different chirality tubes, which may limit the phenyl diazonium functionalization in improving device performance of SWNT network TFTs. To establish how effective the electronically selective chemical functionalization may be when applied to a random network of SWNTs, we now compare the reactivity of several metallic and semiconducting tubes.

Figure 5 shows the ratio of DM to TM in the Raman spectra for metallic and semiconducting tubes as a function of the concentration of 4-BBDT. The chiralities of the tubes are assigned from their RBMs.^{36–38} Semiconducting or metallic classification of tubes without chirality assignment are made from the gate dependence in the electrical measurements. Each type of symbol corresponds to a specific tube measured at different concentrations (e.g., filled square corresponds to DM to TM intensity ratio for one (18,0) tube measured at different concentrations). On average, there is a clear preference for

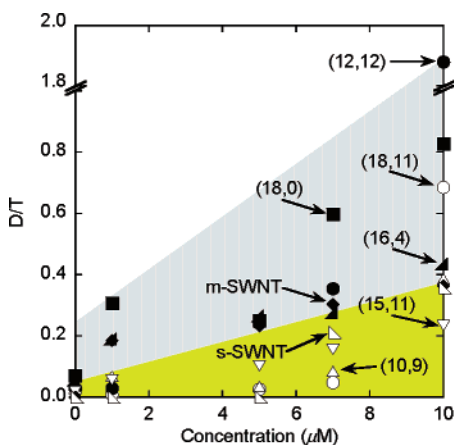


Figure 5. The ratio of the intensities of the DM to TM of eight different SWNTs as a function of 4-bromobenzene tetrafluoroborate concentration. Filled symbols are metallic, and open symbols are semiconducting tubes. Each type of symbol corresponds to a specific tube with the indicated chiral index, which is assigned from the radial breathing mode. Two tubes labeled m-SWNT (metallic) and s-SWNT (semiconducting) are assigned from electrostatic gate dependence of the conductivity. The two different shades are qualitative guides to the eye to show a significant difference between metallic and semiconducting tubes. Note that only the semiconducting (18, 11) tube exhibits significantly higher reactivity at 10 μM compared to other semiconducting tubes investigated.

reaction with metallic tubes (filled symbols) with a very small region of overlap between metallic and semiconducting (open symbols) tubes. Within the different types of tubes examined here, there is really only one semiconducting tube, the (18,11) tube, with reactivity toward 4-BBDT that overlaps significantly with metallic tubes at a relatively high concentration.

Although this result is promising, the changes in the electrical conductivity with respect to the degree of functionalization need to be considered in determining the effectiveness of the diazonium chemistry in improving SWNT network TFT performance. That is, the maximum degree of metallic tube conductivity suppression without the degradation of semiconducting tubes needs to be determined. In Figure 5, all semiconducting tubes have begun to react when metallic tubes are significantly functionalized (i.e., at 7 μM). From studies on electrically contacted single tubes, the conductance of metallic tubes decreases between 1 and 2 orders of magnitude at 7 μM . At this concentration, there is also a significant decrease in the ON-state conductivity of semiconducting tubes by a factor of $\sim 2\text{--}4$ for the samples studied here. These results indicate that, while there will be an improvement in the device performance by selective diazonium chemistry, it is highly unlikely that this method using 4-BBDT can lead to an ideal improvement where all metallic tubes become completely insulating while the large ON-state conductance of all semiconducting tubes are maintained for a network TFT with a significant chirality distribution.

Response of Short Channel SWNT Network TFTs. With both electrical and Raman responses of isolated metallic and semiconducting SWNTs established, we now discuss the effects of 4-BBDT directly on the performance of SWNT network TFTs. Figure 6 shows the responses of a SWNT random network TFT to chemical reaction with 4-BBDT. The channel length of this device is 1 μm . The average tube length is $\sim 5 \mu\text{m}$. In this short channel limit where the average tube length is significantly longer than the channel length, most tubes directly connect the source and drain electrodes as seen in the

AFM image (inset Figure 6C). The onset of changes in the Raman spectra (Figures 6A and B) and the electrical conductance (Figure 6C) of this device is at $\sim 5 \mu\text{M}$ concentration of 4-BBDT. The disappearance of the RBM, the decrease in the intensity of TM, and the appearance of DM for a (13,1) tube within the channel are accompanied by the decrease in both ON and OFF currents. However, no significant changes in the Raman spectrum of a semiconducting (17,6) tube in the same device are observed at this concentration (middle spectrum in Figure 6B). The magnitudes of the decrease in the ON and OFF currents are essentially identical (1.8 μA decrease for the ON current and 2 μA decrease for the OFF current) for the reaction at this concentration. At higher concentration of $\sim 10 \mu\text{M}$, both metallic and semiconducting tubes are functionalized (parts A and B of Figure 6 top spectra), and there is a further drop in the ON current without much change in the OFF current leading to the degradation rather than improvement in performance.

Comparison of the transfer characteristics plotted in the linear scale (Figure 6D) for this device before and after the reaction with 5 μM 4-BBDT reveals that the transconductance does not change significantly. The average of the forward and the reverse sweep transconductance is 104 nA/V before the reaction and 116 nA/V after. The effective device mobility is given by $\mu_{\text{device}} \approx |\partial I_{\text{D}}/\partial V_{\text{G}}|L/WCV_{\text{D}}$, where I_{D} is the drain current, V_{G} is the gate voltage, L is the channel length, W is the channel width, and V_{D} is the drain voltage. Following ref 10, we estimate the gate capacitance, C , to be $\sim 8.6 \times 10^{-5} \text{ F/m}^2$ from the relation $C \approx \epsilon\epsilon_0/t$ where ϵ is the dielectric constant of the gate oxide (3.9), ϵ_0 is the vacuum permittivity, and t is the oxide thickness (400 nm). With $L = 1 \mu\text{m}$, $W = 10 \mu\text{m}$ (i.e., the entire channel width), and $V_{\text{D}} = 100 \text{ mV}$, the device mobility before and after the reaction with 5 μM 4-BBDT is 12 and 13 cm^2/Vs , respectively. On the basis of the average density of $\sim 3 \mu\text{m}^{-2}$ and the tube diameter range of $\sim 1\text{--}3 \text{ nm}$, we estimate the fill factor (i.e., percentage of the area covered by tubes) to be $\sim 0.6\%$. These estimates lead to per tube mobilities of ~ 2000 and $\sim 2200 \text{ cm}^2/\text{Vs}$ before and after reaction, respectively. Therefore, no significant change in the mobility accompanies the same amount of decrease of the ON and the OFF currents upon reaction with 5 μM 4-BBDT.

These observations can be explained by considering the relative length scales of the tubes and the device channel. The channel length of the device (1 μm) is significantly shorter than the average tube length ($\sim 5 \mu\text{m}$). Therefore, most tubes directly span the full length of the channel (inset Figure 6C). As a simple approximation, we can consider the tubes to be all in parallel. Then the overall conductance is simply the sum of the individual tube conductance. In this scenario, when the metallic tubes react with 4-BBDT and the semiconducting tubes do not, the decrease in the overall conductance should reflect only the decrease in the conductance of the metallic tubes. Since the metallic tubes do not exhibit any gate dependence, the decrease in the ON and the OFF currents should have equal magnitudes. This is indeed what we observe in Figure 6C. No change in the mobility combined with the same decrease in the ON and the OFF currents upon reaction with 5 μM 4-BBDT suggests that this may be the ideal situation where only metallic tubes have reacted. However, most devices exhibit less than this ideal behavior (i.e., a larger decrease in the ON current than the OFF current with some decrease in the mobility), most likely due to

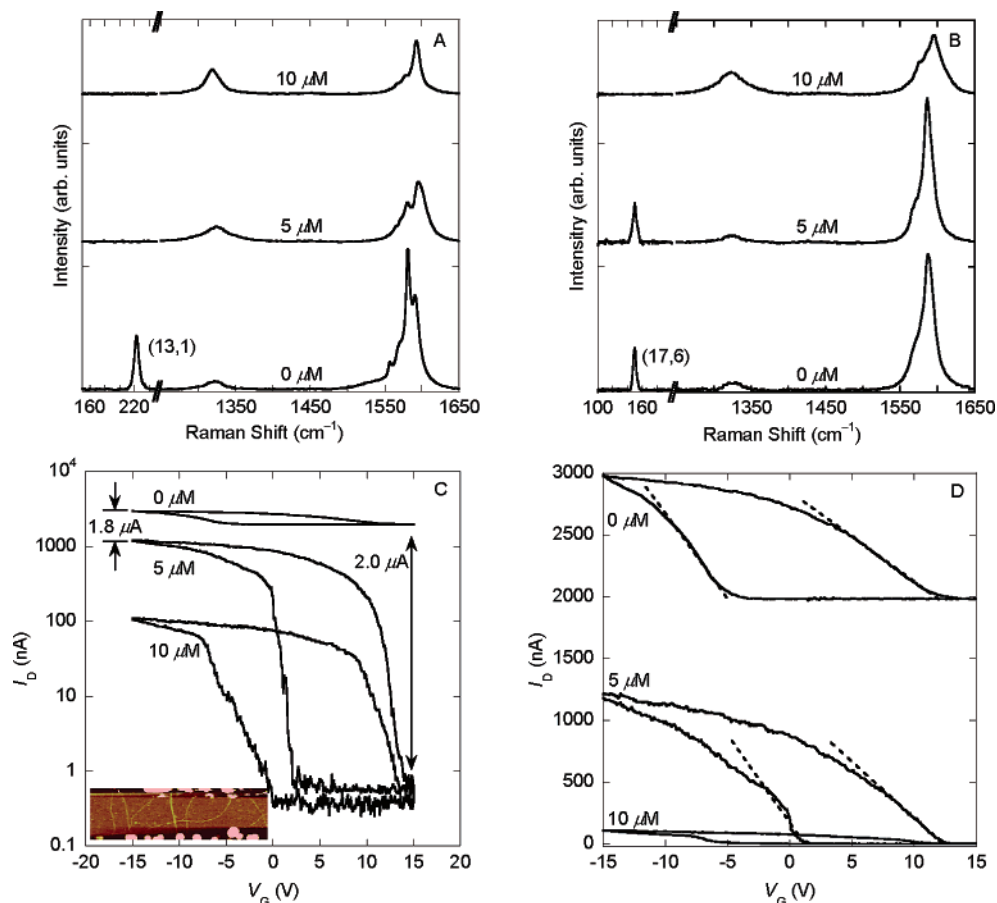


Figure 6. (A) Raman spectra of a metallic tube within a 1- μm channel length SWNT TFT before and after functionalization at the indicated concentrations. Note that there may be two tubes resonant at this spot based on the TM. However, the single RBM peak corresponds to a metallic tube. (B) Raman spectra of a semiconducting tube at a different location of the same SWNT TFT before and after functionalization. $V_{\text{DS}} = 100$ mV. (C) Transfer characteristics of the same device before and after functionalization. $V_{\text{DS}} = 100$ mV. The inset is an AFM image of a portion of the device showing that most tubes directly span the drain and the source electrodes (1 μm separation). (D) Figure 6C plotted in linear scale. Dashed lines are guides to the eye illustrating the forward and reverse transconductance of the device.

the fact that considerable degradation/reaction of semiconducting tubes occurs at conditions in which a significant suppression of metallic tube conductivity is achieved as discussed earlier. Upon further reaction at higher concentrations, semiconducting tubes are also covalently functionalized and a larger decrease in the ON current without much change in the OFF current and a reduction of the carrier mobility are expected and are observed in parts C and D of Figure 6.

Long Channel Length SWNT Network TFTs. Parts A and B of Figure 7 show the Raman spectra of a metallic and a semiconducting tube within a 55- μm channel length network device before and after the reaction with 4-BBDT at the indicated concentrations. Similar Raman signature and therefore the reactivity with 4-BBDT where the metallic tube responds at a lower concentration than the semiconducting one as observed for isolated single tubes are seen. The transfer characteristics at the corresponding concentrations are shown in Figure 7C. Although the metallic tube has reacted to the point where the DM has larger intensity than the TM, there is no significant change in the conductance until the reaction is carried out at 10 μM 4-BBDT concentration when a significant amount of reaction takes place for both metallic and semiconducting tubes. At this concentration, there is nearly an order of magnitude decrease in both the ON current and the transcon-

ductance. The OFF current is less than 100 pA to begin with and remains negligible upon reaction.

In the limit of long channel lengths (i.e., when the channel length is significantly longer than the average tube length), network behavior where every current pathway has at least one intertube junction is expected. With average tube length of ~ 5 μm , there is likely to be about 10 or more junctions in each conduction path. It is also highly unlikely to have an all-metal pathway. With an expected distribution of $\sim 2:1$ ratio of semiconducting to metallic tubes, every conduction path is likely to contain at least one semiconducting tube in this long channel limit. If each conduction path in the network can be considered to contain tubes in series, then the highest resistance component will dominate the overall conductance of that pathway. When the semiconducting tube is turned off by the electrostatic gate, it should in principle have the highest resistance. The OFF current is then determined by the behavior of the semiconducting tubes as confirmed by the current depletion at positive gate voltages in the transfer characteristics of the as-fabricated 55- μm channel length device (Figure 7C).

The contribution of each conduction pathway to the global ON current, on the other hand, may be limited by the junction resistance between metallic and semiconducting tubes which should present the highest resistance component when semi-

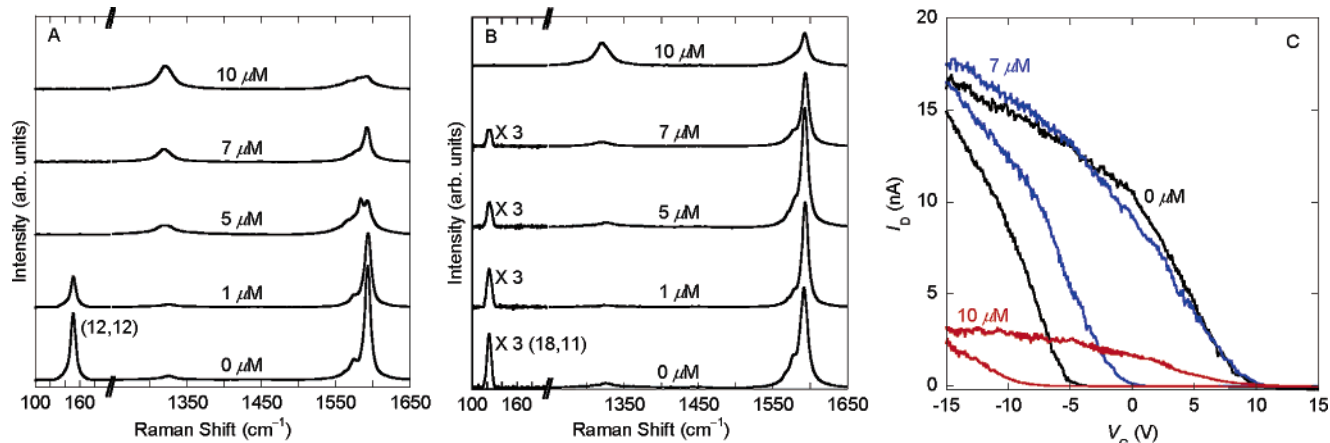


Figure 7. (A) Raman spectra of a metallic tube within the channel region of a 55- μm channel length SWNT film device before and after treatment with the indicated concentrations of 4-BBDT. (B) Raman spectra of a semiconducting tube at a different location within the channel of the same device upon functionalization. (C) Changes in the transfer characteristics of the same SWNT TFT upon reaction with 4-BBDT. $V_{\text{DS}} = 100$ mV.

conducting tubes are turned on. Since the resistance of the junction between metallic and semiconducting tubes has been measured to be about 2 orders of magnitude higher than metal–metal and semiconductor–semiconductor junctions and three or more orders of magnitude higher than intratube resistance,⁴⁰ we assume that the contribution of each conduction path containing at least one metallic tube to the overall ON current is limited by the metal–semiconductor junction resistance. The fact that the global ON current of the long channel device does not decrease after the reaction with 4-BBDT up to 7 μM concentration where significant reaction presumably takes place on metallic tubes is consistent with the picture where the metal–semiconductor junctions limit the ON current conductance of pathways containing at least one metallic tube. On the basis of the results from single-tube transistors, 7 μM 4-BBDT should reduce the conductance of metallic tubes by about 1–2 orders of magnitude and the semiconducting tubes by less than 1 order of magnitude (i.e., the metal–semiconductor junction resistance is still the highest resistance). The ON current of the mixed metal–semiconductor pathway should start to decrease only when the resistance of metallic tubes or semiconducting tubes that are turned on exceed the metal–semiconductor junction resistance. This is consistent with the observations in Figure 7C where a significant drop in the global ON current is seen only at 4-BBDT concentration of ~ 10 μM and higher.

However, the same onset of global ON current decrease at the point where significant amount of semiconducting tubes have reacted can also be explained by the fact that there may be a significant number of all-semiconductor pathways. If all-semiconductor and mixed semiconductor–metal conduction pathways may be considered to be in parallel, the larger conductance pathway (i.e., the all-semiconductor pathways) dominates the global ON-state conductance. In this case, the global ON current will, of course, decrease when semiconducting tubes have reacted significantly and the changes in the mixed metal–semiconductor pathways may be negligible. However, in both types of conduction paths, the starting point of the global ON current decrease should be where significant functionalization has occurred for both metallic and semiconducting tubes.

Insights into whether the major contribution to the global ON current change is determined by metal–semiconductor junctions or the all-semiconductor pathways may be gained from the comparison of changes in the mobilities of the short and the long channel devices. There is nearly an order of magnitude decrease in the transconductance from 1.6 to 0.3 nA/V at the onset of conductivity change (upon reaction with 10 μM 4-BBDT) as seen in Figure 7C for the long channel TFT. In contrast, there is no decrease in the transconductance of the short channel device at the onset of the ON current decrease as shown in Figure 6D. From an analysis similar to that described earlier for the short channel device, we estimate the effective device mobility to be about 5 and 1 cm^2/Vs before and after the reaction for the long channel TFT. With a fill factor of $\sim 0.3\%$, the corresponding effective per tube mobilities are ~ 1700 and ~ 300 cm^2/Vs . This fill factor is only one-half of the value for the short channel device because half of the tubes in the channel are removed by striping in the long channel TFTs. Prior to the chemical treatment, the effective device mobility is about a factor of 2 smaller than the short channel TFT. The effective per tube mobility, on the other hand, is only slightly smaller for the long channel. This suggests that, whether the electrical conduction is through a tube directly spanning the channel or through one or more tube–tube junctions, the mobility is similar. Since the metal–semiconductor junction imposes large resistances, these mobility values are more consistent with the case where the long channel device contains one or more all-semiconductor pathways that dominate the global ON current. Further studies are needed and are underway to address specific contributions from different types of conduction pathways to the observed changes due to chemical functionalization.

Conclusion

We have shown that 4-BBDT can selectively react with SWNTs as well as SWNT devices fabricated on SiO_2/Si substrates. Whether the tubes are electrically contacted or not, the Raman signature and therefore the chemical reactivity remains the same. Correlation between Raman spectral and electrical responses upon reaction with 4-BBDT has been made on isolated tubes which in turn can explain the behavior of random networks of different channel lengths. On average, there is a preference for metallic tubes to react with 4-BBDT. Although there is a

(40) Fuhrer, M. S.; Nygard, J.; Shih, L.; Forero, M.; Yoon, Y. G.; Mazzone, M. S. C.; Choi, H. J.; Ihm, J.; Louie, S. G.; Zettl, A.; McEuen, P. L. *Science* **2000**, *288*, 494–497.

distribution of reactivity (with respect to concentration dependence), the overlap region between metallic and semiconducting tubes is very small indicating substantial selectivity. However, significant suppression of metallic tube conductivity by reaction with 4-BBDT requires concentrations at which considerable reaction occurs for most semiconducting tubes. These observations explain the limitations of the device performance improvement in SWNT random network TFTs with 4-BBDT. The ideal case where the magnitude of the OFF current decrease is the same as the decrease in the ON current while the device mobility (as well as the high per tube mobility) is maintained has been

observed only in the short channel limit where direct connections rather than intertube network behavior dominates.

Acknowledgment. This work was supported by the NSF (Grant No. NIRT-0403489 and DMR-0348585), ACS PRF, and DARPA-funded AFRL-managed Macroelectronics Program Contract FA8650-04-C-7101. We made use of the facilities at the Center for Microanalysis of Materials, University of Illinois, which is partially supported by the U.S. Department of Energy under Grant DEFG02-91-ER45439.

JA0526564